JOURNAL OF GUIDANCE, CONTROL, AND DYNAMICS
Vol. 21, No. 4, July–August 1998

Planar Dynamics of Flexible Manipulators with Slewing Deployable Links

M. Caron,* V. J. Modi,† S. Pradhan,‡ and C. W. de Silva§
University of British Columbia, Vancouver, British Columbia V6T 1Z4, Canada
and
A. K. Misra¶
McGill University, Montreal, Quebec H3A 2K6, Canada

Space manipulators present several features uncommon to ground-based robots: They are highly flexible, are often mobile, and have a degree of redundancy. As space robots become more complex, efficient algorithms are required for their simulation and control. The present study uses an order N algorithm, based on the Lagrangian approach and velocity transformations, to simulate the planar dynamics of an orbiting manipulator with arbitrary number of slewing and deployable flexible links. The relatively general formulation accounts for interactions between orbital, librational, slewing, deployment, and vibrational degrees of freedom and, thus, is applicable to a large class of manipulator systems of contemporary interest. A parametric analysis of the system dynamics suggests significant coupling between the rigid-body motion and structural vibrations. Obviously, this would affect the manipulator's performance. A nonlinear controller based on the feedback linearization technique is developed to regulate the rigid degrees of freedom.

Nomenclature

$\boldsymbol{D}_i$	= vector describing the position of F_i relative to F_0
$\boldsymbol{d}_i$	= translation of the frame F_i from the tip of the $(i\text{th} - 1)$ body
$\mathrm{d}m_i$	= mass of the infinitesimal element located on the ith body
EA_i, EI_i	= structural stiffness of the ith body in the longitudinal and transverse directions, respectively
$\boldsymbol{e}_i$	= displacement of F_i due to bending of the $(i\text{th} - 1)$ body
$\boldsymbol{F}$	= vector containing the forcing terms associated with centrifugal, Coriolis, gravitational, and elastic forces
F_i	= reference frame attached to the ith body
F_0	= inertial reference frame
$\boldsymbol{f}_i$	= displacement of the mass element located at $\boldsymbol{r}_i$ due to structural flexibility
$\boldsymbol{I}^a$	= $a \times a$ identity matrix
K_i	= torsional stiffness of the ith joint
$\boldsymbol{K}_p, \boldsymbol{K}_v$	= position and velocity gain matrices, respectively
l_i	= length of the ith body
$\boldsymbol{M}, \tilde{\boldsymbol{M}}$	= coupled and decoupled system mass matrices, respectively
m_i	= mass of the ith body
N	= number of bodies considered in a given study
$\mathcal{O}(N)$	= order N
$\boldsymbol{Q}$	= vector containing the controlled components of $\boldsymbol{q}$
$\boldsymbol{q}$	= set of generalized coordinates leading to the coupled mass matrix $\boldsymbol{M}$
$\tilde{\boldsymbol{q}}$	= set of generalized coordinates leading to the decoupled mass matrix $\tilde{\boldsymbol{M}}$
$\boldsymbol{q}_c$	= vector containing the controlled components of $\boldsymbol{q}$
$\boldsymbol{q}_d$	= desired values for $\boldsymbol{q}_c$
$\boldsymbol{q}_s$	= vector containing the specified components of $\boldsymbol{q}$
$\boldsymbol{R}, \boldsymbol{R}^C, \boldsymbol{R}^V$	= transformation matrices relating $\dot{\boldsymbol{q}}$ and $\dot{\tilde{\boldsymbol{q}}}$
$\boldsymbol{r}_i$	= position vector of the elemental mass $\mathrm{d}m_i$ with respect to F_i
r_o	= distance of the platform's center of mass from the inertial reference frame F_0
$\boldsymbol{T}_i$	= matrix describing the rotation of F_i relative to F_0
$\boldsymbol{u}$	= vector containing the control inputs
u_i, v_i	= longitudinal and transverse components of $\boldsymbol{f}_i$, respectively
x_i, y_i	= Cartesian components of $\boldsymbol{r}_i$
α_i	= controlled rotation of F_i
β_i	= rotation of F_i due to the elastic deformation of joint i
$\boldsymbol{\delta}_i$	= vector of time-dependent generalized coordinates describing the elastic deformation of the ith body
η_i	= inertial orientation of the ith actuator rotor
θ	= true anomaly of the system
$\boldsymbol{\Lambda}$	= vector containing the Lagrange multipliers
ξ_i	= rotation of F_i due to bending of body $i - 1$
$\boldsymbol{\Phi}_i$	= matrix containing admissible shape functions for the ith body
ψ_i	= angle describing the orientation of F_i relative to F_0

Superscripts

	= total differentiation with respect to time
T	= transpose of the matrix

Presented as Paper 96-3625 at the AIAA/AAS Astrodynamics Specialist Conference, San Diego, CA, July 29–31, 1996; received Nov. 11, 1996; revision received Jan. 22, 1998; accepted for publication Jan. 29, 1998.

*Natural Sciences and Engineering Research Council Graduate Fellow, Department of Mechanical Engineering.

†Professor Emeritus, Department of Mechanical Engineering. Fellow AIAA.

‡Postdoctoral Fellow, Department of Mechanical Engineering. Member AIAA.

§Natural Sciences and Engineering Research Council Chair Professor of Industrial Automation, Department of Mechanical Engineering.

¶Professor, Department of Mechanical Engineering. Associate Fellow AIAA.

I. Introduction

SPACE robotic systems, such as the remote manipulator system on the Space Shuttle, can be used for a variety of purposes including the deployment, retrieval, inspection, construction, repair, and maintenance of satellites, space stations, and experimental payloads. They can also serve as platforms for astronauts during extravehicular activities and can assist in docking maneuvers, for instance, between a Space Shuttle and an orbiting platform.

Space manipulators, as well as large flexible space structures in general, have unveiled a new and challenging field of dynamics and control. As robotic manipulators are slowly gaining importance in space operations, understanding the dynamics and control of large flexible structures capable of varying their geometric configuration is also receiving more attention. Over the years, a large body of literature has evolved, which has been reviewed quite effectively by a number of authors including Meirovitch and Kwak,[1] Modi,[2] Modi and Shrivastava,[3] and Nagata et al.[4]

Space manipulators are significantly different from their ground-based counterparts[5]: They are not attached to a fixed base but are supported by an orbiting platform. The dynamics of the manipulator and the supporting base are coupled. This is usually undesirable; however, it can be used to advantage in attitude control of the platform.[6] Other key differences include the highly flexible character of the links on space-based manipulators, as well as large payload-to-manipulator mass ratios. This may lead to significant structural vibrations. Furthermore, presence of redundancy is often desirable to cope with partial failure or obstacles in the path of the manipulator. The redundancy can also be used, quite effectively, in isolating the dynamics of the platform from the disturbances induced by manipulator maneuvers.[7] The equations governing the dynamics of the robotic systems just described are highly nonlinear, nonautonomous, and coupled and can be expressed in the general form

$$M(q,t)\ddot{q} + F(\dot{q},q,t) = Q(\dot{q},q,t) \tag{1}$$

where $M(q,t)$ is the system mass matrix; $F(\dot{q},q,t)$ contains the terms associated with the centrifugal, Coriolis, gravitational, and elastic forces; and $Q(\dot{q},q,t)$ represents nonconservative generalized forces, including the control inputs.

Equation (1) describes the inverse dynamics of the system. For simulations, forward dynamics of the system is required, and Eq. (1) must be solved for $\ddot{q}$,

$$\ddot{q} = M^{-1}(Q - F) \tag{2}$$

The solution of these equations of motion generally requires $\mathcal{O}(N^3)$ arithmetic operations, where N represents the number of bodies considered in a study. In other words, the number of computations required by an $\mathcal{O}(N^3)$ algorithm will vary with the cube of the number of bodies. Clearly, the computational cost can become prohibitive for a large N. Hence, development of an $\mathcal{O}(N)$ algorithm, where the number of arithmetic operations increases linearly with the number of bodies in the system, has been the focus of several studies in the field of multibody dynamics.[8–14] Such algorithms reduce the computational time and memory requirements considerably, making real-time applications possible.

The Newton–Euler formulation has been used extensively in the past for ground-based robots.[8] It is inherently of $\mathcal{O}(N)$, and the computational efficiency has made it an attractive choice for dynamical simulation studies and control of robots. Although the traditional Lagrange formulation is of $\mathcal{O}(N^4)$, Hollerbach[9] has proposed a recursive $\mathcal{O}(N)$ Lagrangian formulation for the inverse dynamics of rigid-multibody systems. It is not as efficient as its Newton–Euler counterpart, yet it makes real-time applications possible with the Lagrangian approach. It should be noted that the forward dynamics of the same model is not of $\mathcal{O}(N)$. Keat[10] has used a velocity transformation approach to obtain an $\mathcal{O}(N)$ algorithm describing the dynamics of flexible-multibody systems. Rosenthal[11] has based his $\mathcal{O}(N)$ formulation, which considers rigid bodies, on Kane's equations. Jain and Rodriguez[12] use the filtering and smoothing approach of optimal estimation and have introduced spatial operators to obtain a recursive $\mathcal{O}(N)$ formulation for flexible-multibody systems.

Most $\mathcal{O}(N)$ formulations reported in the literature are recursive: They rely on a series of forward and backward passes along the chain of bodies to compute the accelerations and forces in the system. However, Kurdila et al.[13] have proposed a nonrecursive formulation, based on the range space method, which has its basis in finite element solution procedures. The main advantage of a nonrecursive formulation is that the computations for each body can be executed independently, making it suitable for parallel processing. Pradhan et al.[14] have introduced another nonrecursive formulation procedure for flexible-multibody systems, which uses the Lagrangian approach

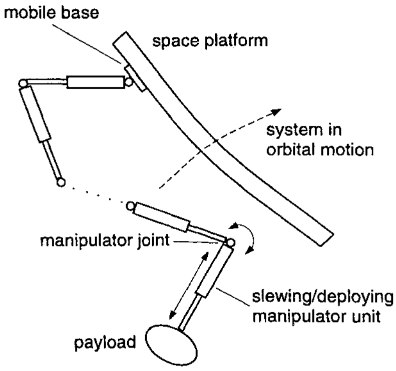

Fig. 1 Schematic diagram of a mobile flexible deployable manipulator, based on a space platform, considered for study.

in conjunction with two velocity transformations. The velocity transforms decompose the system mass matrix into a product of matrices. The inversion of this new form of the mass matrix is computationally far less intensive. As most arithmetic operations in Eq. (2) arise from the inversion of the mass matrix, the resulting algorithm is of $\mathcal{O}(N)$ and, hence, considerably more efficient.

In the present investigation, an efficient mathematical model is developed for studying the in-plane dynamics and control of a general, flexible, space-based manipulator (Fig. 1). The governing equations of motion for this system are derived using the $\mathcal{O}(N)$ approach mentioned.[14] The formulation is extended to include cases where the length of each body is taken as a generalized coordinate and to account for flexible joints. Thus, the mathematical model and the associated computer code represent versatile tools for the dynamical study and, more importantly, in the development of control strategies for flexible space manipulators.[15] A parametric study illustrates the effectiveness of the approach in tackling representative problems of contemporary interest. Finally, the performance of a nonlinear control strategy, based on the feedback linearization technique (FLT), is assessed in regulating this class of systems.[16]

II. Description of the System

The general nature of the model presented here allows for serial manipulators consisting of an arbitrary number N of flexible, slewing, and deployable units (Fig. 1). The formulation provides for arbitrary variation of geometric, inertia, and stiffness characteristics along the manipulator. In the present study, manipulator units are assumed to be interconnected through revolute joints. However, combinations of revolute and prismatic joints can also be considered. The model accounts for flexibility and dissipation at the manipulator joints. The manipulator is taken to be located on a mobile base, which is free to translate along an orbiting space platform. The coupling effects between the orbital, librational, slew, deployment, and vibrational degrees of freedom, associated with the platform and manipulator, are also taken into account.

An essential feature of the model is the time-varying length of each unit, with prismatic joints providing the deployment degrees of freedom. In other words, each of the manipulator units can be deployed and retrieved independently, thereby changing the librational and vibrational characteristics of the overall system. Thus, the manipulator units consist of two telescopic links, each with its own spatially varying properties. Note, the model considered here is rather general and is applicable to a large class of mobile flexible manipulators based on an orbiting space platform.[15] A number of studies reported in the literature become particular cases of the present model.[17]

Because they are relatively small, the elastic deformations of the manipulator and platform are discretized using assumed modes for each component of the system.[18] Deformation of the ith body is expressed as the product of spatially varying admissible shape functions Φ_i and time-dependent generalized coordinates δ_i. Thus, the elastic displacement of the ith body can be expressed as

$$\begin{bmatrix} u_i \\ v_i \end{bmatrix} = \begin{bmatrix} \Phi_{ix} & 0 \\ 0 & \Phi_{iy} \end{bmatrix} \begin{bmatrix} \delta_{ix} \\ \delta_{iy} \end{bmatrix} = \Phi_i \delta_i \tag{3}$$

where u_i and v_i are the longitudinal and transverse elastic displacements, respectively, of an elemental mass located on the ith body at $\boldsymbol{r}_i$. Similarly, the subscripts x and y refer to the longitudinal and transverse modes of vibration, respectively. Thus, $\Phi_i \in \Re^{2\times(r+s)}$ and $\delta_i \in \Re^{(r+s)}$, where r and s are the number of modes considered in the longitudinal and transverse directions, respectively.

Although the formulation accounts for the longitudinal elastic deformation, this study focuses on the transverse displacements. The platform is assumed to behave as a free-free Euler–Bernoulli beam, whereas the links are considered to be Euler–Bernoulli cantilever beams with tip masses. For the transverse vibration of the ith body, the admissible shape functions for the kth mode take the form

$$\Phi_{iyk}(x_i, l_i) = A_{ik1}\sin\left(\frac{\lambda_{ik}x_i}{l_i}\right) + A_{ik2}\cos\left(\frac{\lambda_{ik}x_i}{l_i}\right) + A_{ik3}\sinh\left(\frac{\lambda_{ik}x_i}{l_i}\right) + A_{ik4}\cosh\left(\frac{\lambda_{ik}x_i}{l_i}\right) \tag{4}$$

where x_i is the position along l_i and the A_{ikj} and λ_{ik} depend on boundary conditions of the ith body. It must be emphasized that, because l_i is taken as a generalized coordinate, the shape functions vary with time.

III. Formulation of Problem

A. Kinematics of the System

The multibody system considered for study is an open chain, as shown in Fig. 2. F_0 is the inertial reference frame located at the center of mass of the Earth, and F_i is the body-fixed frame attached to the ith body. The position of an elemental mass $\mathrm{d}m_i$, located on the body i, can be described with respect to the inertial reference as

$$\boldsymbol{R}_{\mathrm{d}m_i} = \boldsymbol{D}_i + \boldsymbol{T}_i\{\boldsymbol{r}_i + \boldsymbol{f}_i(\boldsymbol{r}_i)\} \tag{5}$$

where $\boldsymbol{r}_i$ is the rigid component of the position vector of the elemental mass $\mathrm{d}m_i$ in the frame F_i with $\boldsymbol{r}_i = [x_i, y_i]^T$ and $\boldsymbol{f}_i$ represents the displacement due to the flexibility of the body with $\boldsymbol{f}_i = [u_i, v_i]^T$.

If the position and orientation of the body-fixed frames are known relative to the inertial frame, in addition to the length and elastic deformation of each body, the kinematics of the system is completely described. The position of F_i can be specified directly relative to the inertial frame by $\boldsymbol{D}_i$ and, similarly, its orientation by an inertial angle ψ_i, as shown in Fig. 3a. Note, the rotation matrix $\boldsymbol{T}_i$ can be expressed as

$$\boldsymbol{T}_i = \begin{bmatrix} \cos\psi_i & -\sin\psi_i \\ \sin\psi_i & \cos\psi_i \end{bmatrix} \tag{6}$$

An alternate way to describe a body-fixed frame is to define it with respect to the previous frame. With this methodology, the frame F_i is related to the frame F_{i-1} (Fig. 2). F_i can be obtained by translating F_{i-1} along the length $\boldsymbol{l}_{i-1}$ of the $(i\text{th}-1)$ body and then along $\boldsymbol{d}_i$ where $\boldsymbol{d}_i$ represents the translation of F_i from the tip of the body $i-1$ due to a prismatic joint. Finally, F_i is translated along $\boldsymbol{e}_i$,

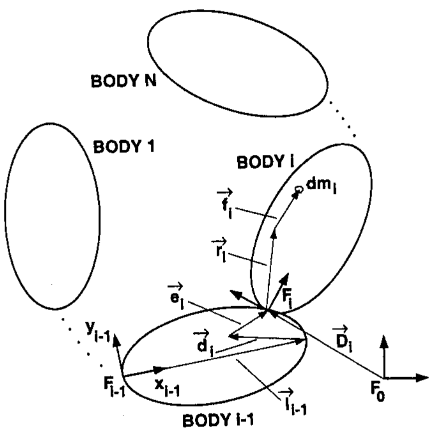

Fig. 2 Schematic diagram of a multibody system in chain topology: coordinate frames and vectors used to define an elemental mass.

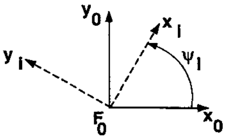

a) Relative to the inertial reference

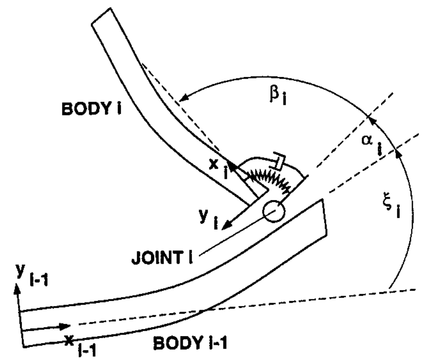

b) Relative to the preceding frames

Fig. 3 Orientation of body-fixed frames.

which is the displacement caused by the elastic deformation of the $(i\text{th}-1)$ body. Rotation of the frame F_i with respect to the frame F_{i-1} has three contributions (Fig. 3b): elastic deformation of body $i-1$ in the transverse direction (ξ_i); rotation of the actuator rotor (α_i), which corresponds to the controlled rotation of the revolute joint; and elastic deformation of joint i (β_i), which could be due, for instance, to flexible coupling. Therefore,

$$\boldsymbol{D}_i = \boldsymbol{D}_{i-1} + \boldsymbol{T}_{i-1}(\boldsymbol{l}_{i-1} + \boldsymbol{d}_i + \bar{\Phi}_{i-1}\delta_{i-1}) \tag{7}$$

and

$$\psi_i = \psi_{i-1} + \xi_i + \alpha_i + \beta_i \tag{8}$$

Thus, the position of F_i is expressed in terms of that of F_{i-1}, which itself is related to the location of F_{i-2}. This referencing with respect to the preceding frame continues until the frame F_1 is reached, which is directly described relative to the inertial frame by $\boldsymbol{D}_1$ and ψ_1. Thus,

$$\boldsymbol{D}_i = \boldsymbol{d}_1 + \sum_{j=2}^{i} \boldsymbol{T}_{j-1}(\boldsymbol{l}_{j-1} + \boldsymbol{d}_j + \bar{\Phi}_{j-1}\delta_{j-1}) \tag{9}$$

where $\boldsymbol{d}_1 = \boldsymbol{D}_1$ and $\bar{\Phi}_{i-1} = \Phi_{i-1}$ evaluated at $\boldsymbol{l}_{i-1} + \boldsymbol{d}_i$. Note that $\boldsymbol{D}_1$ is expressed in polar coordinates

$$\boldsymbol{D}_1 = \begin{bmatrix} r_o\cos\theta \\ r_o\sin\theta \end{bmatrix} \tag{10}$$

where r_o is the orbital radius of the first body.

For convenience, it was decided to describe explicitly the orbital motion of the center of mass of the first body instead of that of the center of mass of the entire system. Because the first body will usually represent a space platform, it will normally constitute most of the mass of the system. Hence, the center of mass of the entire system will lie close to the platform's center of mass. Nevertheless, it should be emphasized that the effects of the motion of the system's center of mass, due to the rigid and flexible degrees of freedom of all the bodies, are accounted for in this formulation.

Thus, two sets of generalized coordinates are available for the complete description of the motion of the system: $\tilde{\boldsymbol{q}}$ and $\boldsymbol{q}$. They are defined as

$$\tilde{\boldsymbol{q}} = \begin{bmatrix} \tilde{q}_1 \\ \tilde{q}_2 \\ \tilde{q}_3 \\ \vdots \\ \tilde{q}_N \end{bmatrix} \in \Re^{n_s}, \qquad \text{with} \qquad \tilde{q}_i = \begin{bmatrix} \boldsymbol{D}_i \\ \eta_i \\ \psi_i \\ \delta_i \\ l_i \end{bmatrix} \in \Re^{n_b} \tag{11}$$

and

$$q = \begin{bmatrix} q_1 \\ q_2 \\ q_3 \\ \vdots \\ q_N \end{bmatrix} \in \Re^{n_s} \quad \text{with} \quad q_i = \begin{bmatrix} d_i \\ \alpha_i \\ \psi_i \\ \delta_i \\ l_i \end{bmatrix} \in \Re^{n_b} \tag{12}$$

Each body is described by $n_b = 5 + r + s$ generalized coordinates and the total number of degrees of freedom for the system is $n_s = Nn_b$. Both sets have ψ_i, δ_i, and l_i as generalized coordinates. In the first set, where D_i and η_i (with $\eta_i = \psi_{i-1} + \xi_i + \alpha_i$) are taken as generalized coordinates, the dynamics of each body is described independently, without referring to adjacent bodies. Consequently, the derivation of the kinetic and potential energies of the system becomes quite simple. On the other hand, the constraints required to specify some generalized coordinates can be quite complicated. The second set, with its recursive definition of the frames, complicates the derivation of the system kinetic and potential energies, but simplifies the constraints. Therefore, the methodology consists in deriving the system energy using the decoupled set of coordinates defined in Eq. (11) and then converting it to the more convenient coupled set, which is defined by Eq. (12). This can be done through the use of the following two velocity transformations. The first velocity transformation is

$$\dot{\bar{q}} = R^V \dot{q} \tag{13}$$

where

$$R^V = \begin{bmatrix} R_1 & 0 & 0 & \cdots & 0 \\ R_1^A & R_2 & 0 & \cdots & 0 \\ R_1^B & R_2^A & R_3 & \cdots & 0 \\ \vdots & \vdots & \vdots & \ddots & \vdots \\ R_1^B & R_2^B & R_3^B & \cdots & R_N \end{bmatrix} \tag{14}$$

with

$$R_i = \begin{bmatrix} T_{i-1}S_i & 0 & 0 & 0 & 0 \\ \xi_{i,d}[1 \quad 0] & 1 & 0 & 0 & 0 \\ 0 & 0 & 1 & 0 & 0 \\ 0 & 0 & 0 & I^{(r+s)} & 0 \\ 0 & 0 & 0 & 0 & 1 \end{bmatrix} \tag{15}$$

$$R_i^A = \begin{bmatrix} T_{i-1}S_i & 0 & Pg_{i+1} & T_i\bar{\Phi}_i & T_i\begin{bmatrix} 1 \\ v_{i+1,l} \end{bmatrix} \\ 0 & 0 & 1 & \bar{\Phi}_i' & \xi_{i+1,l} \\ 0 & 0 & 0 & 0 & 0 \\ 0 & 0 & 0 & 0 & 0 \\ 0 & 0 & 0 & 0 & 0 \end{bmatrix} \tag{16}$$

$$R_i^B = \begin{bmatrix} T_{i-1}S_i & 0 & Pg_{i+1} & T_i\bar{\Phi}_i & T_i\begin{bmatrix} 1 \\ v_{i+1,l} \end{bmatrix} \\ 0 & 0 & 0 & 0 & 0 \\ 0 & 0 & 0 & 0 & 0 \\ 0 & 0 & 0 & 0 & 0 \\ 0 & 0 & 0 & 0 & 0 \end{bmatrix} \tag{17}$$

$$S_i = \begin{bmatrix} 1 & 0 \\ v_{i,d} & 1 \end{bmatrix}, \quad \text{and} \quad P = \begin{bmatrix} 0 & -1 \\ 1 & 0 \end{bmatrix} \tag{18}$$

Here $R^v \in \Re^{n_s \times n_s}$; $\bar{R}_i, R_i^A, R_i^B \in \Re^{n_b \times n_b}$; $g_{i+1} = T_i(l_i + d_{i+1} + e_{i+1})$; $I^j = j \times j$ identity matrix; $T_0 = I^2$; and $v_{1,d} = \xi_{1,d} = 0$. The other velocity transformation can be written as

$$\dot{\bar{q}} = [I^{n_s} - R^C]^{-1} R\dot{q} \tag{19}$$

where

$$R = \begin{bmatrix} R_1 & 0 & 0 & \cdots & 0 \\ 0 & R_2 & 0 & \cdots & 0 \\ 0 & 0 & R_3 & \cdots & 0 \\ \vdots & \vdots & \vdots & \ddots & \vdots \\ 0 & 0 & 0 & \cdots & R_N \end{bmatrix} \tag{20}$$

$$R^C = \begin{bmatrix} 0 & 0 & 0 & 0 & \cdots & 0 \\ R_1^C & 0 & 0 & 0 & \cdots & 0 \\ 0 & R_2^C & 0 & 0 & \cdots & 0 \\ 0 & 0 & R_3^C & 0 & \cdots & 0 \\ \vdots & \vdots & \vdots & \vdots & \ddots & \vdots \\ 0 & 0 & 0 & 0 & \cdots & 0 \end{bmatrix} \tag{21}$$

$$R_i^C = \begin{bmatrix} I^2 & 0 & Pg_{i+1} & T_i\bar{\Phi}_i & T_i\begin{bmatrix} 1 \\ v_{i+1,l} \end{bmatrix} \\ 0 & 0 & 1 & \bar{\Phi}_i' & \xi_{i+1,l} \\ 0 & 0 & 0 & 0 & 0 \\ 0 & 0 & 0 & 0 & 0 \\ 0 & 0 & 0 & 0 & 0 \end{bmatrix} \tag{22}$$

Here $R, R^C \in \Re^{n_s \times n_s}$ and $R_i^C \in \Re^{n_b \times n_b}$.

B. Kinetic Energy of the System

The total kinetic energy of the system can be written as

$$T = \sum_{i=1}^{N} \frac{1}{2} \int_{m_i} \dot{R}_{dm_i} \cdot \dot{R}_{dm_i} \mathrm{d}m_i \tag{23}$$

which can be expressed in the quadratic form

$$T = \tfrac{1}{2} \dot{\bar{q}}^T \tilde{M} \dot{\bar{q}} \tag{24}$$

where $\tilde{M}$ is the $n_s \times n_s$ mass matrix expressed in terms of the decoupled set of generalized coordinates

$$\tilde{M} = \begin{bmatrix} \tilde{M}_1 & 0 & 0 & \cdots & 0 \\ 0 & \tilde{M}_2 & 0 & \cdots & 0 \\ 0 & 0 & \tilde{M}_3 & \cdots & 0 \\ \vdots & \vdots & \vdots & \ddots & \vdots \\ 0 & 0 & 0 & \cdots & \tilde{M}_N \end{bmatrix} \tag{25}$$

However, using the two velocity transformations described earlier, the kinetic energy can be expressed in terms of the second set of generalized coordinates [Eq. (12)]. Therefore, making use of Eq. (13), the kinetic energy expression takes the form

$$T = \tfrac{1}{2} \dot{q}^T \underbrace{R^{V^T} \tilde{M} R^V}_{M} \dot{q} \tag{26}$$

But using Eq. (19) one has

$$T = \tfrac{1}{2} \dot{q}^T \underbrace{R^T [I^{n_s} - R^C]^{-T} \tilde{M} [I^{n_s} - R^C]^{-1} R}_{M} \dot{q} \tag{27}$$

where the kinetic energy of the system, as well as the mass matrix M, are both expressed in terms of the second set of generalized coordinates. Note that the inverse of the mass matrix, as defined in Eq. (27), has the form

$$M^{-1} = R^{-1} [I^{n_s} - R^C] \tilde{M}^{-1} [I^{n_s} - R^C]^T R^{-T} \tag{28}$$

Now the matrices inverted in Eq. (28), i.e., R and $\tilde{M}$, are both block diagonal; thus, their inversion is an $\mathcal{O}(N)$ process. Furthermore, the structure of the remaining matrices in Eq. (28) allows their multiplication to be also of $\mathcal{O}(N)$. Thus, inversion of the system mass matrix, in terms of the second set of generalized coordinates, is now an $\mathcal{O}(N)$ process.

C. Potential Energy

The total gravitational potential energy of the system can be written as

$$V_g = -\sum_{i=1}^{N} \int_{m_i} \frac{\mu\, \mathrm{d}m_i}{R_{\mathrm{d}m_i}} = -\sum_{i=1}^{N} \int_{m_i} \frac{\mu\, \mathrm{d}m_i}{|\boldsymbol{D}_i + \boldsymbol{r}_i + \boldsymbol{f}_i|} \tag{29}$$

where $\mu = Gm_e$, with G the universal gravitational constant and m_e the mass of the Earth. Because the geometrical dimensions of the orbiting system are much smaller than the orbital radius, the integrand was expanded binomially and terms up to the third order in D_i were retained, integrated over each body, and then summed over the number of bodies to obtain the total gravitational energy of the system.

Potential energy is also stored in the elastic deformation of the system. The total elastic potential energy is given by

$$V_e = \sum_{i=2}^{N} \frac{1}{2} K_i \beta_i^2 + \sum_{i=1}^{N} \frac{1}{2} \int_{l_i} EA(x_i) \left(\frac{\partial u_i}{\partial x_i} \right)^2 \mathrm{d}x_i + \sum_{i=1}^{N} \frac{1}{2} \int_{l_i} EI(x_i) \left(\frac{\partial^2 v_i}{\partial x_i^2} \right)^2 \mathrm{d}x_i \tag{30}$$

where the first term represents the contribution from the deformation of the joints; the second and third terms correspond to the elastic deformation of the platform and manipulator links in the longitudinal and transverse directions, respectively; and $\beta_i = \psi_i - \alpha_i - \xi_i - \psi_{i-1}$. Note, both EA and EI are permitted to vary along the length of a given body.

D. Equations of Motion

The equations of motion can be obtained using the Lagrangian procedure

$$\frac{\mathrm{d}}{\mathrm{d}t}\left(\frac{\partial T}{\partial \dot{\boldsymbol{q}}} \right) - \frac{\partial T}{\partial \boldsymbol{q}} + \frac{\partial V}{\partial \boldsymbol{q}} = \boldsymbol{Q} \tag{31}$$

In the present study, $\boldsymbol{Q}$ corresponds to the torques applied by the control momentum gyros, joint actuators, as well as forces applied by the linear actuators responsible for link deployment. The generalized forces can also represent environmentally induced forces resulting in thermal deformations, aerodynamic drag, solar radiation pressure, etc.

The equations of motion can be rewritten as

$$\ddot{\boldsymbol{q}} = \boldsymbol{M}^{-1} \left(\boldsymbol{Q} - \dot{\boldsymbol{M}} \dot{\boldsymbol{q}} + \frac{1}{2} \frac{\partial (\dot{\boldsymbol{q}}^T \boldsymbol{M} \dot{\boldsymbol{q}})}{\partial \boldsymbol{q}} - \frac{\partial V_g}{\partial \boldsymbol{q}} - \frac{\partial V_e}{\partial \boldsymbol{q}} \right) \tag{32}$$

where V_g and V_e are defined in Eqs. (29) and (30), respectively; Eq. (28) is used for $\boldsymbol{M}^{-1}$, and $\boldsymbol{M}$ is as described in Eq. (26).

E. Specified Coordinates

In this study, the coordinates required to describe the system kinematics are taken to be generalized coordinates to make the formulation as general and versatile as possible. However, it is often useful to specify some of these generalized coordinates. For instance, in the particular case of the manipulator studied, $d_i = 0$ for $i = 3, \ldots, N$. In other words, each manipulator link is attached to the tip of the previous link in the chain. Furthermore, cases where the length of the units is varied in a specified manner, or where joint rotors are locked in place at a specified angle, require the use of specified coordinates. These coordinates are prescribed by constraint relations, which are introduced in the equations of motion through Lagrange multipliers. Therefore, when constrained, Eq. (1) takes the form

$$\boldsymbol{M}\ddot{\boldsymbol{q}} + \boldsymbol{F} = \boldsymbol{Q}^d \boldsymbol{u} + \boldsymbol{P}^c \boldsymbol{\Lambda} \tag{33}$$

where $\boldsymbol{u} \in \Re^{n_a}$ is a vector containing the n_a actuator forces and torques, $\boldsymbol{Q}^d$ is the matrix assigning the components of $\boldsymbol{u}$ to the actuated variables ($\boldsymbol{Q} = \boldsymbol{Q}^d \boldsymbol{u}$), $\boldsymbol{\Lambda} \in \Re^{n_c}$ is the vector containing the n_c Lagrange multipliers, and $\boldsymbol{P}^c$ is the matrix assigning the multipliers to the constrained equations. To find the values of the Lagrange multipliers and achieve the desired constraints, Eq. (33) can be rewritten in the form

$$\ddot{\boldsymbol{q}} + \boldsymbol{F}^g - \boldsymbol{F}^u \boldsymbol{u} = \boldsymbol{F}^s \boldsymbol{\Lambda} \tag{34}$$

where $\boldsymbol{F}^g = \boldsymbol{M}^{-1}\boldsymbol{F}$, $\boldsymbol{F}^u = \boldsymbol{M}^{-1}\boldsymbol{Q}^d$, and $\boldsymbol{F}^s = \boldsymbol{M}^{-1}\boldsymbol{P}^c$. Separating the specified variables $\boldsymbol{q}_s$ from the generalized ones ($\boldsymbol{q}_g$) gives

$$\begin{bmatrix} \ddot{\boldsymbol{q}}_g \\ \ddot{\boldsymbol{q}}_s \end{bmatrix} + \begin{bmatrix} \boldsymbol{F}_g^g \\ \boldsymbol{F}_s^g \end{bmatrix} - \begin{bmatrix} \boldsymbol{F}_g^u \\ \boldsymbol{F}_s^u \end{bmatrix} \boldsymbol{u} = \begin{bmatrix} \boldsymbol{F}_g^s \\ \boldsymbol{F}_s^s \end{bmatrix} \boldsymbol{\Lambda} \tag{35}$$

From the equation associated with the specified coordinates, the Lagrange multipliers can be determined:

$$\ddot{\boldsymbol{q}}_s + \boldsymbol{F}_s^g - \boldsymbol{F}_s^u \boldsymbol{u} = \boldsymbol{F}_s^s \boldsymbol{\Lambda} \tag{36}$$

i.e.,

$$\boldsymbol{\Lambda} = \boldsymbol{F}_s^{s-1} \left(\ddot{\boldsymbol{q}}_s + \boldsymbol{F}_s^g - \boldsymbol{F}_s^u \boldsymbol{u} \right) \tag{37}$$

The equations of motion still retain their $\mathcal{O}(N)$ character, even in the presence of constraints, as the Lagrange multipliers can be obtained recursively.[14] Thus, in the case where the jth variable is constrained to be constant at its initial value, $\ddot{q}_{sj} = 0$. In the case of prescribed maneuvers, $\ddot{q}_{sj}$ is simply defined as the desired acceleration profile. In the present study, a sine-ramp profile is adopted for prescribed maneuvers. It assures zero velocity and acceleration at the beginning and end of the maneuver, thereby reducing the structural response of the system. The maneuver time history considered is as follows:

$$q_{sj}(\tau) = (\Delta q_{sj}/\Delta\tau)\{\tau - (\Delta\tau/2\pi)\sin[(2\pi/\Delta\tau)\tau]\} \tag{38}$$

where q_{sj} is the constrained coordinate, Δq_{sj} is its desired variation, τ is the time, and $\Delta\tau$ is the time required for the maneuver.

IV. Dynamical Simulations

A Fortran program was written for the dynamical simulation of the system described in Secs. II and III. The acceleration vector $\ddot{\boldsymbol{q}}$ was integrated numerically using Gear's method, which is well suited for stiff systems of ordinary differential equations.[19] To reduce computational time during simulations, a symbolic manipulation routine (MAPLE V) was used to obtain analytical expressions for the integrals of the shape functions. Furthermore, efficient matrix multiplication algorithms were developed to take advantage of the structure of the various matrices involved.[15]

For the numerical simulation, a space platform, supporting a mobile manipulator, orbiting around the Earth was considered (Fig. 1). The numerical data used in the analysis are summarized as follows: The orbit is circular at an altitude of 400 km with a period of 92.5 min. The geometry of the platform is cylindrical, with axial to transverse inertia ratio of 0.005; mass = 120,000 kg, length = 120 m, and flexural rigidity (EI_p) = 5.5×10^8 Nm^2. The manipulator revolute joint mass = 20 kg, moment of inertia = 10 kg m^2, and stiffness (K) = 1×10^4 Nm/rad. The manipulator links (slewing and deployable) have a cylindrical geometry with axial to transverse inertia ratio of 0.005, mass = 200 kg, length = 7.5 m, and flexural rigidity (EI_s, EI_d) = 5.5×10^5 Nm^2.

In the following simulations, the longitudinal elastic deformation of the bodies is neglected, as well as the dynamics of the mobile base. Furthermore, unless otherwise specified, the manipulator is not supporting any payload, the platform is initially oriented along the local vertical, i.e., $\psi = 0$, and there is no energy dissipation. Finally, as pointed out earlier, the time history of a maneuver is described by Eq. (38).

The first case investigates the response of a one-unit manipulator to the libration and vibration of the supporting platform (Fig. 4). As indicated before, a manipulator unit consists of two telescopic links: One is free to slew and supports the other, which is deployable. The manipulator configuration, important parameters, and initial conditions are also indicated on the figure. The manipulator is supporting a 400-kg-point payload and is located at the extremity of the platform. The slew and deployment joints are both locked in positions (l_2 = 10 m, α_2 = 50 deg). The platform is given an initial pitch disturbance

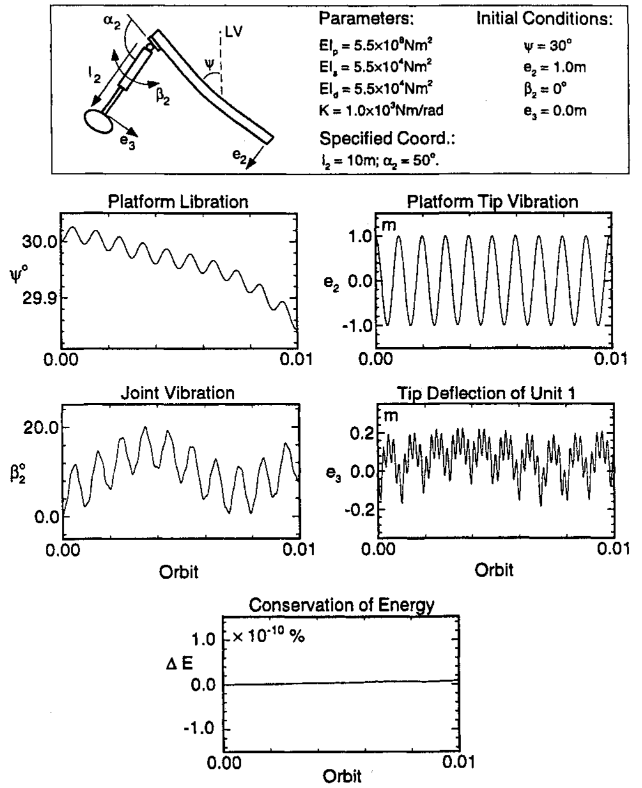

Fig. 4 Response of the one-unit manipulator to libration and vibration of the supporting platform.

of $\psi = 30$ deg and a tip deflection $e_2 = 1$ m. Figure 4 describes the system response to these disturbances. Variation of the total energy of the system, expressed as a percentage of the initial total system energy, is also shown. As can be expected for a conservative system, the energy variation is nearly zero (of the order of $10^{-12}\%$), providing confidence in the formulation and accuracy of the computer code.

Clearly, the joint, link, and platform vibrations, as well as the system pitch librational motion, are coupled. Note, the long-period librational response of the platform is modulated at its vibrational frequency. The same is true with the joint response. It is apparent that the platform dynamics has a significant influence on the manipulator response, which now goes through slewing oscillations with an amplitude approaching 20 deg. Of equal concern are the manipulator's tip oscillations e_3, which clearly show through their modulations the effect of the platform's librational and vibrational dynamics. Obviously, this would affect the tracking performance of the manipulator.

It may be pointed out that the first three modes were used to discretize vibration of the flexible members. The results showed that, in general, use of the fundamental mode is sufficient to describe the structural response. The second mode was found to alter the response only slightly, and the effect of higher modes was rather insignificant. Hence, in the following study, only the first mode is used to represent vibration of a flexible structural member.

The second case examines the effect of link and joint flexibility on the position of the manipulator's end effector (Fig. 5). A five-unit manipulator, i.e., 10 links, 5 free to slew whereas the other 5 are deployable, shown in the inset, is located near the tip of the platform. The individual revolute joints are locked in position as stated in the legend for the diagram (specified coordinates) and so are the deployable links. The platform is subjected to an initial tip deflection of 1 m. As before, although there is a significant transfer of energy between various degrees of freedom, the total energy is conserved. In absence of dissipation, the platform tip oscillations progresses undamped. Here x_e represents the manipulator-tip motion parallel to the undeformed platform, whereas y_e gives the displacement in the transverse direction, both with respect to the reference coordinate frame F_1. To assess the effects of link and joint flexibility, the response with a rigid-manipulator system is also included for comparison. The results clearly show considerable influence of the system flexibility on the position of the end effector. Obviously, this has significant implication on the path planning.

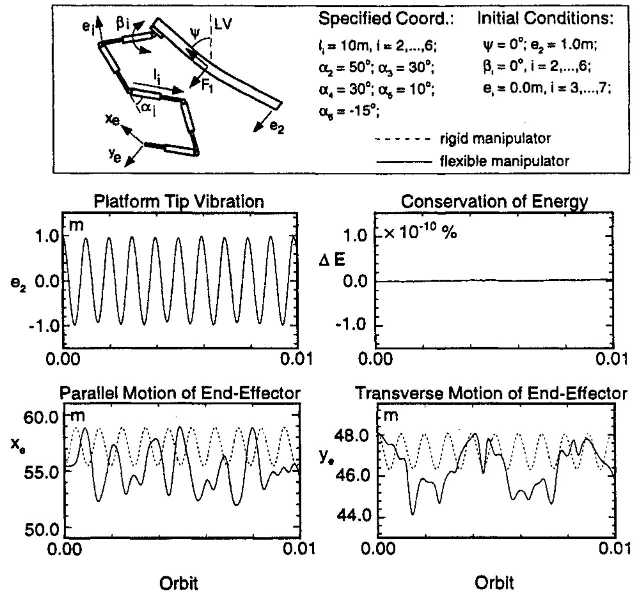

Fig. 5 Effect of link and joint flexibility on the end-effector position for a five-unit manipulator.

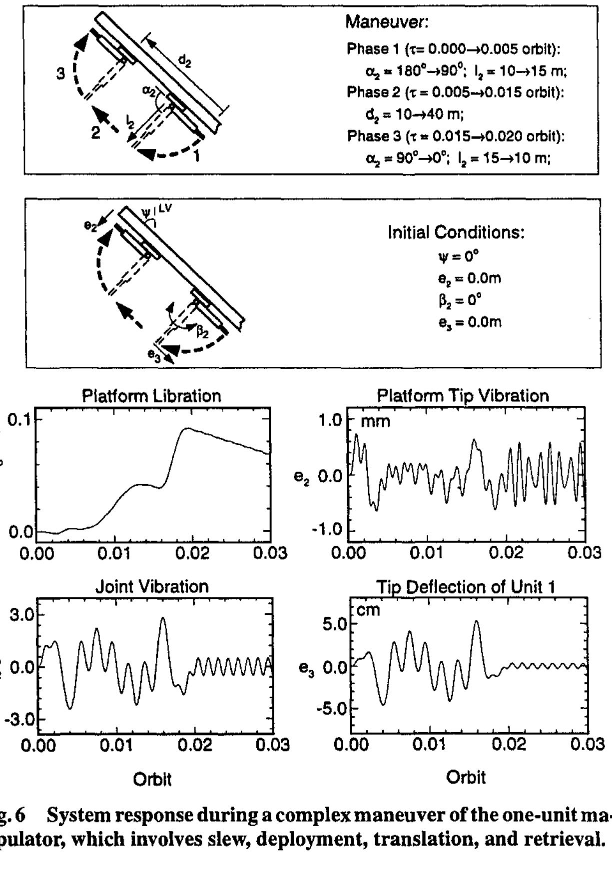

Fig. 6 System response during a complex maneuver of the one-unit manipulator, which involves slew, deployment, translation, and retrieval.

The third case involves a three-phase maneuver with a one-unit manipulator, which is shown in Fig. 6. The first phase (phase 1) consists of a simultaneous rotation and deployment of the manipulator unit. During the second phase (phase 2), the mobile base translates along the platform, with the manipulator unit fully deployed and perpendicular to the platform. The final phase (phase 3) involves simultaneous rotation and retrieval of the manipulator unit. The values for the initial conditions, joint rotations, and deployment lengths are also indicated. The maneuver results in significant vibrations of the slew joint and links, which persist after the end of the maneuver as the system damping is purposely taken to be zero. The

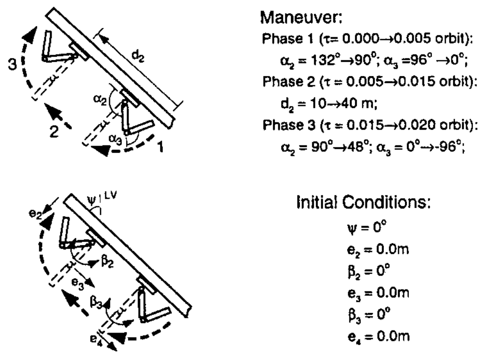

a) Description of initial conditions and maneuver parameters

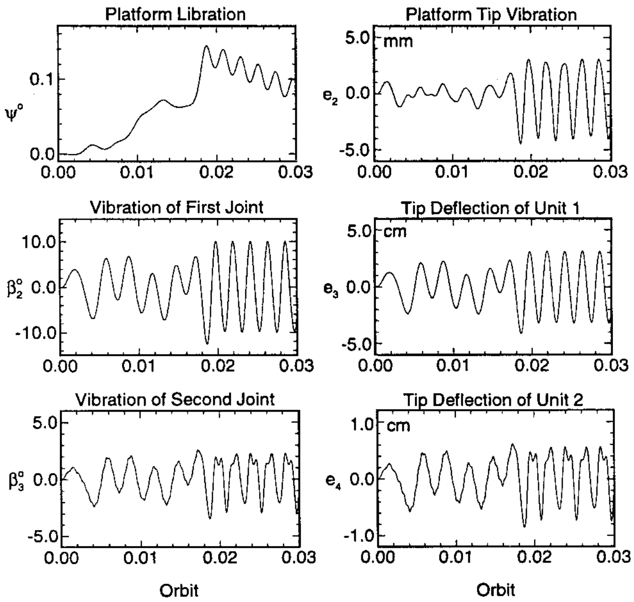

b) Dynamical response of the system

Fig. 7 Three-phase maneuver of a two-unit manipulator involving joint rotations and translation of the mobile base.

maneuver also excites, slightly, the platform vibrational and librational degrees of freedom. Throughout the translation of the mobile base, the manipulator unit is fully deployed, making it more flexible. This can be observed from the response of the manipulator tip: During the translational phase of the maneuver, the lower stiffness of the manipulator unit results in a lower frequency of vibration. After the maneuver, the manipulator unit is partly retracted, thereby increasing its natural frequency.

Finally, response of the system to a similar three-phase maneuver, executed by a two-unit manipulator, is considered (Fig. 7). Both units are fully retracted to their minimum length of 7.5 m and remain so throughout the simulation. The first phase consists of simultaneous slewing maneuvers at both manipulator joints, until the manipulator is fully extended, perpendicular to the platform. During the second phase, the mobile base translates along the platform, with the manipulator remaining normal to the platform. The final phase involves simultaneous rotations at both joints, until the endpoint of the manipulator reaches the platform. The initial conditions and the maneuver time history are indicated in Fig. 7a, whereas the system response is given in Fig. 7b. The larger mass of this two-unit manipulator results in a stronger response in the platform's vibrational and librational degrees of freedom. Note, the vibrational amplitudes for the first joint β_2 and tip deflection of the first unit e_3 are greater than those for the second joint β_3 and second unit e_4. The second unit acts on the first one as a tip mass.

V. Control

The ultimate objective of the dynamical analysis of a system is to control its operational behavior. In other words, find the control input $\boldsymbol{u}$ that will cause the system to behave as desired. In the present case, a controller based on the FLT[16] is designed to regulate the manipulator and platform rigid dynamics. This scheme effectively decouples the system, linearizes it, and uses a proportional-derivative feedback loop to achieve the desired dynamical behavior. The FLT-based controller is designed considering a system consisting of rigid bodies; however, its effectiveness is assessed using the original, fully flexible system.

For a rigid system, Eq. (33) reduces to

$$\boldsymbol{M}_r\ddot{\boldsymbol{q}} + \boldsymbol{F}_r = \boldsymbol{Q}^d_r\boldsymbol{u} + \boldsymbol{P}^c\boldsymbol{\Lambda} \tag{39}$$

where the subscript r indicates that contributions from link flexibility have been removed. Substituting for $\boldsymbol{\Lambda}$ using Eq. (37), Eq. (39) takes the form

$$\boldsymbol{M}_r\ddot{\boldsymbol{q}} + \boldsymbol{F}'r = \boldsymbol{Q}'_{dr}\boldsymbol{u} \tag{40}$$

where $\boldsymbol{F}'_r = \boldsymbol{F}_r - \boldsymbol{P}^c\boldsymbol{F}^{s^{-1}}_{sr}(\ddot{\boldsymbol{q}}_s + \boldsymbol{F}^g_{sr})$, and $\boldsymbol{Q}'_{dr} = \boldsymbol{Q}^d_r - \boldsymbol{P}^c\boldsymbol{F}^{s^{-1}}_{sr}\boldsymbol{F}^u_{sr}$. Solving for $\ddot{\boldsymbol{q}}$ gives

$$\ddot{\boldsymbol{q}} = -\bar{\boldsymbol{F}}'_r + \bar{\boldsymbol{Q}}'_{dr}\boldsymbol{u} \tag{41}$$

where $\bar{\boldsymbol{F}}'_r = \boldsymbol{M}_r^{-1}\boldsymbol{F}_r$ and $\bar{\boldsymbol{Q}}'_{dr} = \boldsymbol{M}_r^{-1}\boldsymbol{Q}'_{dr}$. Equation (41) can be rewritten as

$$\begin{bmatrix} \ddot{\boldsymbol{q}}_c \\ \cdots \\ \ddot{\boldsymbol{q}}_u \end{bmatrix} = -\begin{bmatrix} \bar{\boldsymbol{F}}'_{rc} \\ \cdots \\ \bar{\boldsymbol{F}}'_{ru} \end{bmatrix} + \begin{bmatrix} \bar{\boldsymbol{Q}}'_{drc} \\ \cdots \\ \bar{\boldsymbol{Q}}'_{dru} \end{bmatrix}\boldsymbol{u} \tag{42}$$

where $\boldsymbol{q}_c$ and $\boldsymbol{q}_u$ are the controlled and uncontrolled generalized coordinates, respectively. Considering only the controlled generalized coordinates,

$$\ddot{\boldsymbol{q}}_c = -\bar{\boldsymbol{F}}'_{rc} + \bar{\boldsymbol{Q}}'_{drc}\boldsymbol{u} \tag{43}$$

Equation (43) defines the nonlinear effects inherent in the rigid degrees of freedom. To ensure a robust behavior of the controller, $\ddot{\boldsymbol{q}}_c$ is taken to have the form

$$\ddot{\boldsymbol{q}}_c = \ddot{\boldsymbol{q}}_d + \boldsymbol{K}_v(\dot{\boldsymbol{q}}_d - \dot{\boldsymbol{q}}_c) + \boldsymbol{K}_p(\boldsymbol{q}_d - \boldsymbol{q}_c) \tag{44}$$

where $\boldsymbol{q}_d$ is the desired values for $\boldsymbol{q}_c$, whereas $\boldsymbol{K}_v$ and $\boldsymbol{K}_p$ are the velocity and position controller gain matrices, respectively:

$$\boldsymbol{K}_v = \begin{bmatrix} K_{v1} & 0 & 0 & \cdots & 0 \\ 0 & K_{v2} & 0 & \cdots & 0 \\ 0 & 0 & K_{v3} & \cdots & 0 \\ \vdots & \vdots & \vdots & \ddots & \vdots \\ 0 & 0 & 0 & \cdots & K_{vN} \end{bmatrix} \tag{45}$$

and

$$\boldsymbol{K}_p = \begin{bmatrix} K_{p1} & 0 & 0 & \cdots & 0 \\ 0 & K_{p2} & 0 & \cdots & 0 \\ 0 & 0 & K_{p3} & \cdots & 0 \\ \vdots & \vdots & \vdots & \ddots & \vdots \\ 0 & 0 & 0 & \cdots & K_{pN} \end{bmatrix} \tag{46}$$

Here the diagonal elements of both matrices are scalars selected to satisfy the prescribed requirements of settling time, maximum permissible overshoot, etc. Equating Eqs. (43) and (44) and solving for the control input $\boldsymbol{u}$ gives

$$\boldsymbol{u} = (\bar{\boldsymbol{Q}}'_{drc})^{-1}\{\bar{\boldsymbol{F}}'_{rc} + \ddot{\boldsymbol{q}}_d + \boldsymbol{K}_v(\dot{\boldsymbol{q}}_d - \dot{\boldsymbol{q}}_c) + \boldsymbol{K}_p(\boldsymbol{q}_d - \boldsymbol{q}_c)\} \tag{47}$$

As pointed out earlier, only the rigid degrees of freedom are controlled here. If required, one can develop an appropriate controller to regulate flexible degrees of freedom as shown by Modi et al.[16]

As an example, consider a manipulator with one unit supported by a flexible platform, as shown in Fig. 8. The platform is initially given a disturbance of 1 deg in pitch from the local horizontal

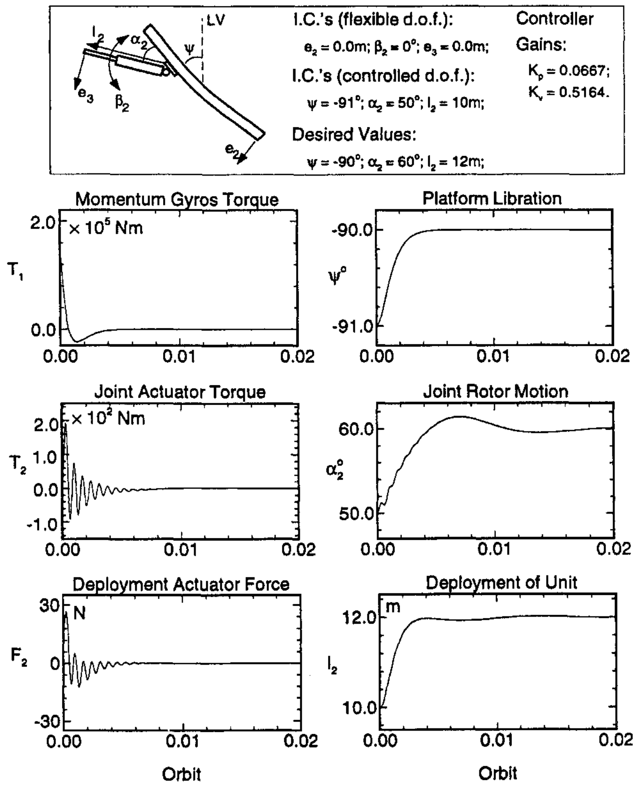

a) Control inputs and response of rigid degrees of freedom

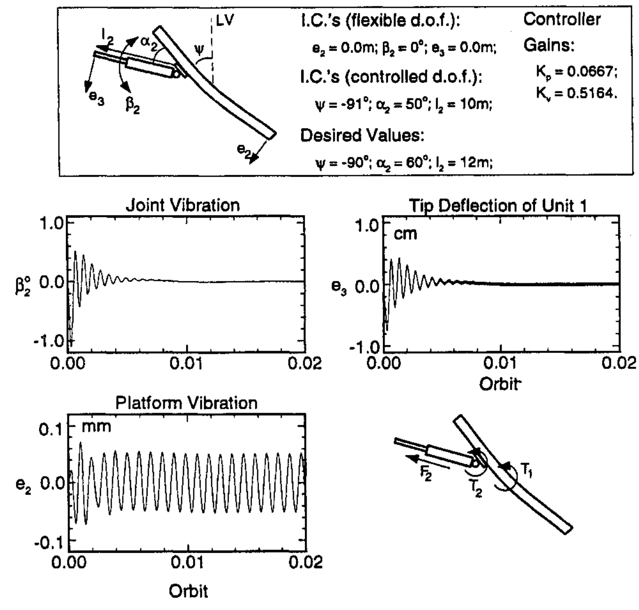

b) Response of flexible degrees of freedom

Fig. 8 Controlled behavior of a one-unit manipulator during a 10-deg slew and 2-m deployment in presence of an initial pitch disturbance of 1 deg.

($\psi = -90$ deg), which now corresponds to the platform's operational orientation. Note, this configuration is inherently unstable if the attitude is left uncontrolled. Simultaneously, the manipulator slews through 10 deg and extends its length by 2 m. For the three control variables, i.e., platform pitch angle, joint rotation, and manipulator length, the proportional and derivative gains are selected to yield a critically damped response q_c, as well as a reduction of the position errors to 2% of their initial values in 0.004 orbit. Figure 8a shows the control input time histories, whereas Fig. 8b gives the system's vibrational response. The initial conditions, desired values for the controlled degrees of freedom, and the controller gains are also given in the legend. The closed-loop response shows the effectiveness of the FLT controller under this demanding situation. Clearly, the unmodeled dynamics of the flexible generalized coordinates affect the performance of the controller. The response of the three controlled variables (ψ, α_2, and l_2) is obviously not critically damped. However, in general, the effect of unmodeled dynamics is small, and the disturbance is damped in less than $\frac{1}{100}$th of an orbit. Even the platform tip vibration, which persists, has an amplitude of only ± 0.2 mm. Obviously, the structural damping, which is purposely not accounted for here, can easily tackle this situation quite effectively. If necessary, one can implement a simple linear vibration control. On the other hand, although not controlled directly, vibration of the manipulator links and the joint are suppressed through coupling between the rigid and flexible degrees of freedom.

VI. Concluding Remarks

The paper presents a rather general formulation for studying in-plane dynamics and control of a manipulator consisting of an arbitrary number of slewing as well as deployable links. The formulation combines the Lagrangian approach with velocity transformations leading to an $\mathcal{O}(N)$ algorithm. This versatile tool can be applied to a large class of systems of contemporary interest. A parametric study suggests coupling between the rigid-body motion and joint as well as link vibrations. In general, the slewing and translational maneuvers have significant effect on the flexible-degrees-of-freedom response. The formulation can be used to obtain critical combinations of the manipulator maneuvers and external excitations that may lead to unacceptable response. For the particular case studied, a controller based on the FLT, which accounts for the complete nonlinear dynamics of the system in the rigid degrees of freedom, is found to be quite effective even in regulating the flexible degrees of freedom through coupling. However, robustness of the controller is an important issue and should receive further attention.

References

[1]Meirovitch, L., and Kwak, M. K., "On the Maneuvering and Control of Space Structures," *Proceedings of the First International Conference on the Dynamics of Flexible Structures in Space* (Cranfield, England, UK), edited by C. L. Kirk and J. L. Junkins, Cranfield Univ., Cranfield, England, UK, 1990, pp. 3–17.

[2]Modi, V. J., "Attitude Dynamics of Satellites with Flexible Appendages—A Brief Review," *Journal of Spacecraft and Rockets*, Vol. 11, No. 11, 1974, pp. 743–751.

[3]Modi, V. J., and Shrivastava, S. K., "Satellite Attitude Dynamics and Control in the Presence of Environmental Torques—A Brief Survey," *Journal of Guidance, Control, and Dynamics*, Vol. 6, No. 6, 1983, pp. 461–471.

[4]Nagata, T., Modi, V. J., and Matsuo, H., "An Approach to Dynamics and Control of Flexible Systems," *A Collection of Technical Papers, AIAA/AAS Astrodynamics Conference*, AIAA, Washington, DC, 1994, pp. 366–375; also AIAA Paper 94-3756, Aug. 1994.

[5]Dubowski, S., and Papadopoulos, E., "The Kinematics, Dynamics, and Control of Free-Flying and Free-Floating Space Robotic Systems," *IEEE Transactions on Robotics and Automation*, Vol. 9, No. 5, 1993, pp. 531–543.

[6]Parlaktuna, O., Cook, G. E., Strauss, A. M., and Fernandez, K. R., "Fine Attitude Control of Space Vehicles Using Space Manipulators," *International Journal of Robotics and Automation*, Vol. 9, No. 1, 1994, pp. 29–35.

[7]Hanson, M. L., and Tolson, R. H., "Reducing Flexible Base Vibrations Through Local Redundancy Resolution," *Journal of Robotic Systems*, Vol. 12, No. 11, 1995, pp. 767–779.

[8]Fu, K. S., Gonzalez, R. C., and Lee, C. S. G., *Robotics: Control, Sensing, Vision, and Intelligence*, McGraw–Hill, New York, 1987, pp. 82–84, 103–124.

[9]Hollerbach, J. M., "A Recursive Lagrangian Formulation of Manipulator Dynamics and a Comparative Study of Dynamics Formulation Complexity," *IEEE Transactions on Systems, Man, and Cybernetics*, Vol. 10, No. 11, 1980, pp. 730–736.

[10]Keat, J. E., "Multibody System Order *n* Dynamics Formulation Based on Velocity Transform Method," *Journal of Guidance, Control, and Dynamics*, Vol. 13, No. 2, 1990, pp. 207–212.

[11]Rosenthal, D. E., "An Order *n* Formulation for Robotic Systems," *Journal of the Astronautical Sciences*, Vol. 38, No. 4, 1990, pp. 511–529.

[12]Jain, A., and Rodriguez, G., "Recursive Flexible Multibody System Dynamics Using Spatial Operators," *Journal of Guidance, Control, and Dynamics*, Vol. 15, No. 6, 1992, pp. 1453–1466.

[13]Kurdila, A. J., Menon, R. G., and Sunkel, J. W., "Nonrecursive Order *N* Formulation of Multibody Dynamics," *Journal of Guidance, Control, and Dynamics*, Vol. 16, No. 5, 1993, pp. 838–844.

[14]Pradhan, S., Modi, V. J., and Misra, A. K., "Order *N* Formulation for Flexible Multibody Systems in Tree Topology—The Lagrangian Approach," *A Collection of Technical Papers, AIAA/AAS Astrodynamics Conference*, AIAA, Reston, VA, 1996, pp. 480–489; also AIAA Paper 96-3624, 1996.

[15]Caron, M., "Planar Dynamics and Control of Space-Based Flexible Manipulators with Slewing and Deployable Links," M.A.Sc. Thesis, Dept. of Mechanical Engineering, Univ. of British Columbia, Vancouver, BC, Canada, Oct. 1996.

[16]Modi, V. J., Karray, F., and Chan, J. K., "On the Control of a Class of Flexible Manipulators Using Feedback Linearization Approach," *Acta Astronautica*, Vol. 29, No. 1, 1993, pp. 17–27; also International Astronautic Federation, Paper IAF-91-324, Oct. 1991.

[17]Modi, V. J., and Ibrahim, A. M., "Dynamics of the Orbiter-Based WISP Experiment," *Acta Astronautica*, Vol. 26, No. 11, 1992, pp. 749–761.

[18]Meirovitch, L., *Elements of Vibration Analysis*, 2nd ed., McGraw–Hill, New York, 1986, pp. 255, 256, 282–290.

[19]Press, W. H., Teukolsky, S. A., Vetterling, W. T., and Flannery, B. P., *Numerical Recipes in FORTRAN*, 2nd ed., Cambridge Univ. Press, Delhi, India, 1992, pp. 727–744.